J Solid State Electrochem (2017) 21:2079–2090
DOI 10.1007/s10008-017-3521-7

ORIGINAL PAPER

Influence of chemical composition and amount of intermixed ionomer in the catalyst on the oxygen reduction reaction characteristics

E. Härk[1,2] · R. Jäger[1] · I. Tallo[1] · U. Joost[3] · P. Möller[1] · T. Romann[1] · R. Kanarbik[1] · V. Steinberg[1] · K. Kirsimäe[4] · E. Lust[1]

Received: 15 November 2016 / Revised: 25 January 2017 / Accepted: 27 January 2017 / Published online: 3 February 2017

Abstract Influence of chemical composition of the ionomers (polyvinyl alcohol (PVA) or Nafion®) on the oxygen reduction reaction (ORR) kinetics has been studied. The 5 wt% Nafion-Vulcan showed higher electrochemical activity toward ORR compared with that for the 5 wt% PVA-Vulcan. Four different Nafion® amounts were used to intermixing a carbide-derived carbon (CDC) or Pt-modified CDC catalysts and the highest electrochemical activity toward ORR was established for the 30 wt% Nafion-Pt/CDC catalyst. Influence of the different amounts of Nafion® ionomer in the catalyst is moderate compared to the effect of variation of the carbon support (Vulcan vs. CDC) or the ionomer (PVA vs. Nafion®). The Randles–Ševcik relationship was used to estimate the effective electrochemical active surface area (S_{eff}) of the electrodes, depending on the chemical composition of the ionomer studied.

Keywords Nafion® ionomer · Polyvinyl alcohol · Carbide-derived carbon · Oxygen reduction reaction · Randles–Ševcik relationship · Effective electrochemical active surface area

E. Härk, R. Jäger, P. Möller, T. Romann and E. Lust are members of ISE.
E. Härk and E. Lust are members of ECS.

✉ E. Lust
enn.lust@ut.ee

[1] Institute of Chemistry, University of Tartu, 14a Ravila Str, 50411 Tartu, Estonia

[2] Soft Matter and Functional Materials, Helmholtz Zentrum Berlin, Hahn-Meitner-Platz 1, 14109 Berlin, Germany

[3] Institute of Physics, University of Tartu, 1 W.Ostwaldi Str, 50411 Tartu, Estonia

[4] Institute of Ecology and Earth Sciences, University of Tartu, 14a Ravila Str, 50411 Tartu, Estonia

Introduction

The properties of the carbon-based electrodes (the specific surface area, porosity, electrical conductivity, ratio of sp^2 and sp^3 hybridized carbon) are influenced by chemical composition and amount of an ionomer in the catalyst [1–7]. It has been recognized that the optimum Nafion® amount varies from 30 to 36 wt%, depending on the platinum content in the catalyst material [4, 8, 9] as well as on the properties of the supportive carbon used. Passalacqua et al. [9] demonstrated that the real active catalyst area in contact with Nafion® ionomer is insufficient to provide adequate electrolytic conductance, if low Nafion® amount (14%) inside a catalyst has been used. On the other hand, if the Nafion® amount in a catalyst is too high, then the catalytically active particles are somewhat more hindered and the interaction of an active site with an oxygen molecule is obstructed [9, 10].

The effects of the carbon supports on the Pt distribution, different perfluorosulfonic acid ionomers and an ionomer coverage on the electrochemical properties were investigated by Park et al. [11, 12]. These investigations led to the conclusion that the ionomer, which covers uniformly and continuously the surfaces of the Pt particles and carbon, improves the efficiency of the catalyst electrocatalytic activity toward oxygen reduction [11, 12].

An intensive research has focused at the same time on the replacement of the Nafion® ionomer due to its poor mechanical stability (brittleness) and non-homogeneous distribution (i.e. differences in the local ion conductivity vs. matrix conductivity) in the fuel cell electrodes [13–15]. Therefore, polyvinyl alcohol (PVA) has been used as a binder in catalyst layer

showing a good film formation capacity, hydrophilic properties and high biodegradability [16–18]. In addition, the current-voltage characteristics for KOH doped PVA membrane-based fuel cell showed higher power compared with the Nafion® ionomer-based classical polymer electrolyte fuel cell [19].

Masa et al. [20], Ward et al. [21, 22] and Menshykau et al. [23] intensively simulated simple electrode processes occurring at stationary, partially active, non-flat electrodes by the rotating disc electrode or voltammetry analysis. Thus, under certain circumstances, the classical Koutecky–Levich and Randles–Ševcik relationships for rough surfaces are justified for analysis.

In this work, the influence of the ionomer chemical composition (PVA vs. Nafion®) and Nafion® ionomer amount (wt%) using an intermixing approach for preparation of the in catalyst ink has been investigated to improve the electrocatalytic activity toward oxygen reduction reaction (ORR) in 0.1M KOH aqueous solution. The platinum nanoparticles modified rough electrode surfaces have been characterized by electrochemical and physical techniques.

Experimental

Materials

The meso-microporous carbide-derived carbon (CDC) powder, synthesized from molybdenum carbide by using the high-temperature chlorination method (at 750 °C) [24], and the Pt nanoparticles modified carbide-derived carbon catalyst (Pt/CDC; 0.2 ± 0.02 mg_{Pt} cm^{-2}) synthesized using the sodium borohydride reduction method [25–30], have been used. Also, the commercially available VulcanXC72-based electrodes (Fuel Cell Earth LLC) were studied.

Preparation of the catalyst ink

Two different ionomers (Nafion®117 (Sigma-Aldrich) or polyvinyl alcohol (PVA, Sigma-Aldrich, M_w 89,000–98,000)) were used as a binder in the catalysts. The catalyst inks were prepared by the intermixing technique, using a carbon powder, PVA or Nafion® ionomer, isopropanol solution (Sigma-Aldrich, >99.0%) and Milli-Q water (18.2 MΩ cm at 25 °C). Received catalyst ink contains 5 wt% of the ionomer (referred to the total electrode weight), noted as 5%PVA-Vulcan or 5%Nafion-Vulcan, respectively. Four different Nafion® amounts (5, 20, 30 and 50 wt%) in the catalyst inks were used for preparation of the unmodified CDC (noted as 5%Nafion-CDC, 20%Nafion-CDC, 30%Nafion-CDC, 50%Nafion-CDC) and Pt/CDC electrodes (noted as 5%Nafion-Pt/CDC, 20%Nafion-Pt/CDC, 30%Nafion-Pt/CDC, 50%Nafion-Pt/CDC). The catalyst suspension (9 μl) was deposited onto the glassy carbon substrate electrode (5 mm diameter, *Pine Instrument Company*).

Physical and electrochemical characterisation techniques

The electrodes (5%PVA-Vulcan and 5%Nafion-Vulcan) were analysed by various physical characterisation methods: the scanning electron microscopy with energy-dispersive X-ray spectroscopy (SEM-EDX, The Helios NanoLab™ 600, FEI), Raman Spectroscopy (Renishaw inVia Raman Microscope with 514 nm laser line), time-of-flight secondary ion mass spectrometry (TOF-SIMS, PHI TRIFT V nanoTOF and using Ga^+ 30 keV primary ions) and X-ray photoelectron spectroscopy (XPS) [30, 31]. The surface station equipped with an electron energy analyser (SCIENTA SES 100) and a non-monochromatic twin anode X-ray tube (Thermo XR3E2) in ultra-high vacuum conditions were used for XPS measurements. The atomic concentrations of different compounds and elements were analysed with Average Matrix Relative Sensitivity Factors procedure [32]. Experimental data were processed by removing of Kα and Kβ satellites, background and the component fitting using Casa XPS software [33]. Thereafter, for fitting of the XPS spectra, Shirley background and the Gauss-Lorentz hybrid function (GL 70, Gauss 30%, Lorentz 70%) were used. Vulcan, unmodified CDC and Pt nanoparticles modified CDC powders were initially characterized by the X-ray diffraction analysis, transmission electron microscopy and nitrogen sorption methods (previously discussed in other publications) [28, 29].

The potentiostat *Reference 600*™ (*Gamry Instruments Inc*) combined with rotating disc electrode (RDE) assembly was applied for the electrochemical measurements. RDE and cyclic voltammetry (CV) measurements were performed at temperature 22 ± 1 °C in 0.1M KOH electrolyte (Sigma-Aldrich, 99.99%) saturated with argon or oxygen. RDE measurements were performed at different electrode rotation rates from 0 to 3000 rev min^{-1} at electrode potential scan rate $\nu = 10$ mV s^{-1}. The cyclic voltammograms were measured at different potential scan rates from 5 to 200 mV $^{-1}$ in Ar or O_2-saturated solutions at the stationary electrode (rotation rate $\omega = 0$ rev min^{-1}). Electrode potentials were measured against the Hg|HgO|0.1 M KOH reference electrode connected to the cell through a long Luggin capillary. At least five independent measurements for every system were carried out and averaged to give the overall result of the study [27–30].

The very high frequency series resistance, obtained from the impedance measurements, was found to be 40 ± 3Ω for 0.1 M KOH solution and was used for iR-drop correction of the measured data [27–30]. Thus, the presented RDE and CV data have been corrected with iR-drop values and background current densities obtained for systems in Ar-saturated 0.1 M KOH solution.

Results and discussion

Physical characteristics for Vulcan-based systems

The scanning electron microscopy with energy-dispersive X-ray spectroscopy data for Vulcan electrode mixed with different ionomers (PVA or Nafion®) demonstrates the similar structure (Fig. 1). The scanning electron microscopy (SEM) images (Fig. 1a, b) for systems studied show that surfaces are quite rough and to the first approximation comparable each other, i.e. both surfaces have the nearly similar structure.

The SEM-EDX data in Fig. 1c, d demonstrate that the exposition of elements depends on the ionomer (PVA or Nafion®) used. For 5%Nafion-Vulcan some fluorine and sulphur (average 2.21 and 0.59 wt%, respectively, from Nafion® binder), oxygen (average 5.6 wt%; probably functional groups containing oxygen on the Vulcan surface), and copper (from sample plate) have been observed. Detailed analysis of the two selected areas of the 5%PVA-Vulcan electrode surface shows that the oxygen amount (average 7.9 wt%) is somewhat higher for 5%PVA-Vulcan than that for the 5%Nafion-Vulcan electrode due to the oxygen in the OH group in PVA.

The detailed analysis of the samples (Vulcan powder, 5%Nafion-Vulcan and 5%PVA-Vulcan) has been conducted using the time-of-flight secondary ion mass spectrometry method within the mass range from 0 to 400 amu z^{-1} (Fig. 2). The negative and positive secondary ions were analysed in areas of 25 × 25 μm^2 using a raster of 512 × 512 measured points. The intensive ^{19}F isotope and $^{38}F_2$ component peaks state clearly the features of the Nafion® ionomer within the 0–50 amu z^{-1} range measured (Fig. 2b), compared to the spectra measured for the Vulcan powder (Fig. 2a). The partial negative TOF-SIMS spectra for 5%PVA-Vulcan electrode (Fig. 2c) show relatively intensive peaks of oxygen isotope and existence of the oxygen containing functional groups in PVA. It should be noted that the both ionomers (PVA and Nafion®) were homogeneously distributed into the Vulcan powder. This result has been confirmed by SEM data, given in Fig. 1c, d.

The X-ray photoelectron spectroscopy was used for investigation of the electronic states and elemental composition of the samples, and influence of the ionomers used (Fig. 3a–c). XPS spectra were collected at a pass energy of 200 eV with a step size 0.5 eV over a binding energy range from 600 to 0 eV (not shown here for shortness). XPS data for Vulcan powder show the presence of carbon (C1s) and oxygen (O1s) within the energy range from 295 to 280 eV (step size = 0.1 eV) (Fig. 3a). In addition, several contributions from different chemical functional groups and carbon electronic configurations can be deconvoluted

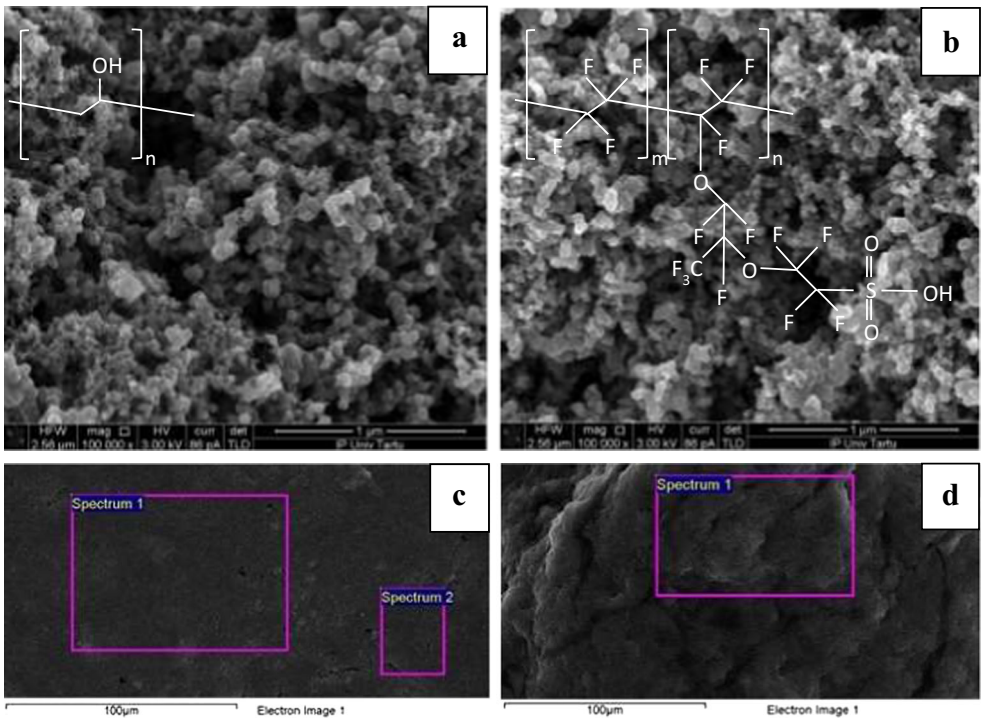

Fig. 1 SEM images (**a**, **b**) and SEM-EDX data (**c**, **d**) for 5%PVA-Vulcan (**a**, **c**) and 5%Nafion-Vulcan (**b**, **d**) deposited onto copper sample plate

5%PVA-Vulcan	C	O	Cu
Spectrum 1	90.02	9.66	0.32
Spectrum 2	92.90	6.76	0.34

5%Nafion-Vulcan	C	O	F	S	Cu
Spectrum 1	90.61	5.60	2.21	0.59	0.98

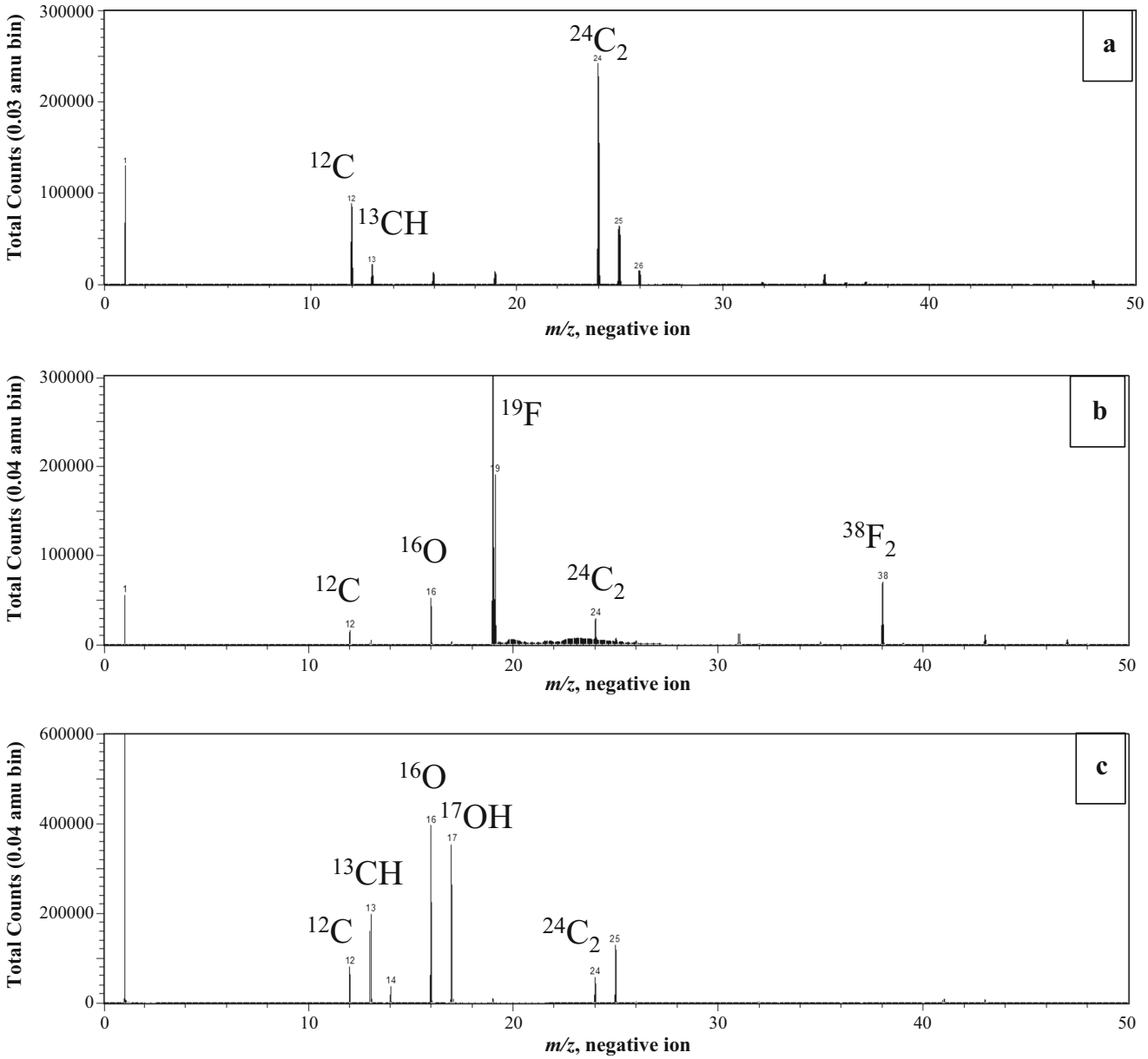

Fig. 2 Partial negative TOF-SIMS spectra within the mass range from 0 to 50 (m/z) of the Vulcan powder (**a**), 5%Nafion-Vulcan (**b**) and 5%PVA-Vulcan (**c**) catalysts

in the C1s spectra [29]. Following oxygen containing species were found in the C1s spectra: C–O (286.4 eV), C = O (287.8 eV), O–C = O (288.2 eV), carbonates (290 eV) and π-π* (291.7 eV) [34–38]. Signals corresponding to sp^2 and sp^3 hybridized carbons can be found at 284.1 and 285.4 eV, respectively (Fig. 3a–c). The ratio between sp^2 and sp^3 hybridized carbon was estimated to be 7:1 in the Vulcan powder, 3:1 in 5%Nafion-Vulcan and 1:1 in 5%PVA-Vulcan-based electrodes, respectively. The increase of the sp^3 hybridized carbon peak intensity in the XPS spectrum is apparent, thus, the change of the sp^2/sp^3 hybridized carbon ratio is influenced by the different distribution characteristics of the ionomers used in the catalyst ink. The additional signal from $-CF_2$ group is presented in the spectra for 5%Nafion-Vulcan (Fig. 3b).

The Raman spectrometry was used for characterisation of prepared inks (5%PVA-Vulcan, 5%Nafion-Vulcan). Neither PVA nor Nafion® ionomer characteristic peaks for residuals were observed at the fixed wavelengths (514 and 785 nm) (e.g. the depth resolution of the Raman spectrometry depends upon the wavelength of the laser used, being ~0.7 at 532 nm), indicating that due to very low wt% of the ionomer mixed in the catalyst ink, there is no formation of the thick ionomer film on the carbon particles [39].

However, it is necessary to emphasize that the ionomer film formation depends significantly on the carbon support

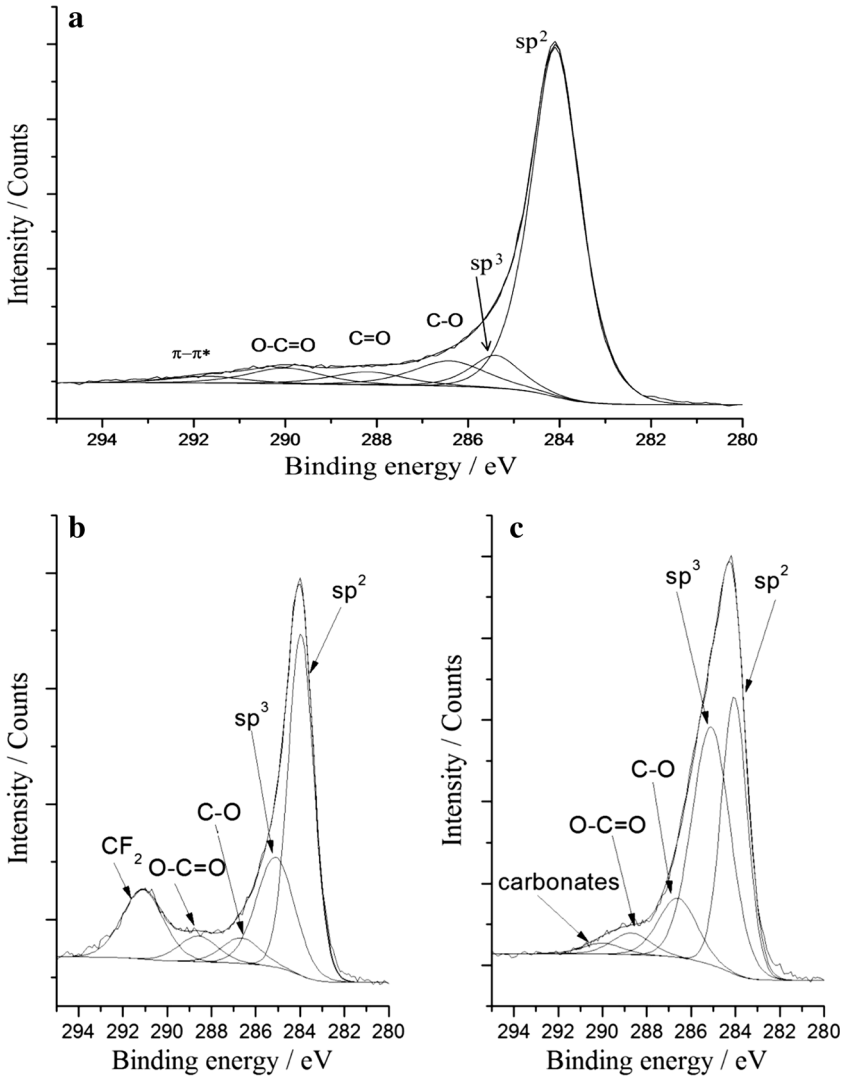

Fig. 3 Detailed XPS spectra of C1s for Vulcan powder (**a**), 5%Nafion-Vulcan (**b**) and 5%PVA-Vulcan (**c**) catalysts

characteristics (e.g. ionophobic/ ionophilic properties) and on the chemical composition of the ionomer used [11].

Detailed physical characterization of CDC and Pt/CDC catalysts has been discussed in our previous works [27–29].

Electrochemical characterisation

Influence of the PVA or Nafion® ionomer on the ORR characteristics

The RDE data (corrected for iR-drop and background current values) for 5%PVA-Vulcan and 5%Nafion-Vulcan electrodes in O_2-saturated 0.1 M KOH solution at the electrode rotation rate $\omega = 500$ rev min^{-1} and at the electrode potential scan rate $\nu = 10$ mV s^{-1} are presented in Fig. 4. The electrochemical activity toward ORR is defined by the ionomer chemical composition used. The half-wave potential value ($E_{1/2}$) for PVA containing electrodes is shifted toward more negative electrode potentials due to changes in the chemical composition and the conductivity of the electrode material studied [40]. The corrected current density value (j_c) at fixed electrode potential ($E = -0.25$ V vs. Hg|HgO|0.1 M KOH) assigned to the mixed kinetic current region is found to be −3.3 and −11.6 A m^{-2} for the 5%PVA-Vulcan and 5%Nafion-Vulcan electrodes, respectively. The j_c values analysed for the 5%Nafion-Vulcan system within diffusion limiting current region showed 1.5 times higher values than that obtained for 5%PVA-Vulcan. The corresponding j_c values at $E = -0.51$ V vs. Hg|HgO|0.1 M KOH are found to be −11.9 and -18.3 A m^{-2} for 5%PVA-Vulcan and 5%Nafion-Vulcan, respectively. Thus, the 5%Nafion-Vulcan system is electrochemically more active toward ORR compared to the 5%PVA-Vulcan electrodes within the electrode potential range from −0.20 to −0.75 V vs. Hg|HgO|0.1 M KOH, due to better electronic and ionic conductivity within Nafion® ionomer-based electrode.

The Tafel-like relationships (inset in Fig. 4) were constructed using the calculated kinetic current density values ($|j_{kin}|$)

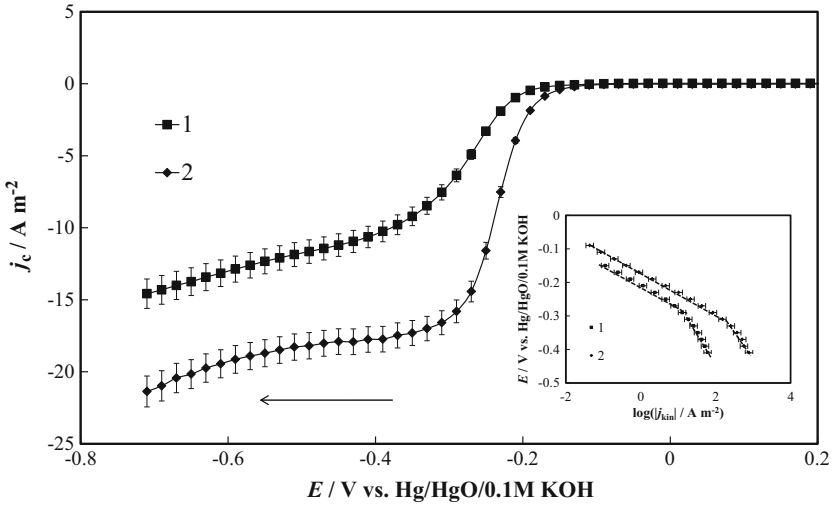

Fig. 4 RDE data for 5%PVA-Vulcan (*1*) and 5%Nafion-Vulcan (*2*) in 0.1 M KOH solution saturated with O_2 ($\nu = 10$ mV s^{-1}, $\omega = 500$ rev min^{-1}). *Inset*: Tafel-like plots for 5%PVA-Vulcan (*1*) and 5%Nafion-Vulcan (*2*)

obtained from the intercept of the Koutecky-Levich (j_c^{-1} vs. $\omega^{-1/2}$) plots. At less negative electrode potentials, the Tafel-like plots for both systems studied are linear with the slope value about −60 mV dec^{-1} independent of the ionomer used. It should be noted that wider (about 60 mV) mixed kinetic current region is established for 5%Nafion-Vulcan (from −0.11 to −0.31 V vs. Hg|HgO|0.1 M KOH) compared with that for the 5%PVA-Vulcan (from −0.13 to −0.27 V vs. Hg|HgO|0.1 M KOH) (inset in Fig. 4) indicating that the multiple-electron transfer process takes place within wider electrode potential range for 5%Nafion-Vulcan. Thus, the improved electronic and ionic conductivity has been achieved by mixing the Nafion® ionomer with the Vulcan powder. In the high current density region, the slope values of the Tafel-like plots change and, therefore, the Langmuir mechanism within the low current density region is replaced by the more complex ORR mechanism [27, 41–45].

The cyclic voltammetry curves for the Vulcan-based systems intermixed with the different ionomers (Nafion® or PVA) show remarkable differences, leading to the conclusion that the chemical composition and most likely the structure of the electrode have a great influence on the catalyst performance (Fig. 5). The Randles–Ševcik relationships are presented in the inset in Fig. 5. The peak current (I_{peak}) vs. $\nu^{1/2}$ plots are linear (i.e. diffusion controlled ORR process takes place) for both electrodes, yet the 5%PVA-Vulcan system shows about four times lower slope value compared to that obtained for the 5%Nafion-Vulcan electrode. For further analysis, the following equation has been used [21]:

$$I_{peak} = -0.496nSFc_{sys}\sqrt{\frac{nF\nu D_{sys}}{RT}}, \quad (1)$$

where n is the number of electrons consumed in the electroreduction ($n = 2$ for Vulcan and CDC or $n = 4$ for Pt/CDC), S is the geometric surface area of a substrate electrode (0.196 cm^2), F is the Faraday constant and α is the electron transfer coefficient ($\alpha = 0.5$). The diffusion coefficient (D_{sys})

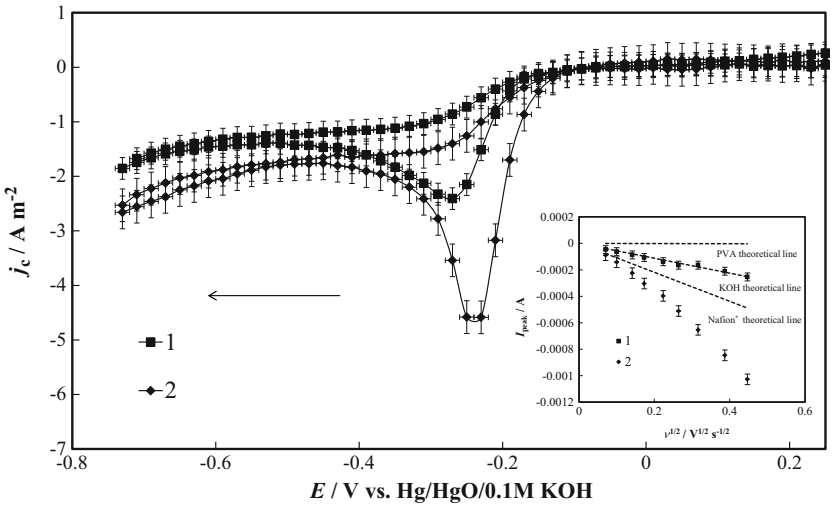

Fig. 5 Cyclic voltammograms for 5%PVA-Vulcan (*1*) and 5%Nafion-Vulcan (*2*) in 0.1 M KOH solution saturated with O_2 and at potential scan rate $\nu = 5$ mV s^{-1}. *Inset*: I_{peak} vs. $\nu^{1/2}$ dependence for 5% PVA-Vulcan (*1*) and 5%Nafion-Vulcan (*2*) in 0.1 M KOH solution saturated with O_2 within potential scan rate range from 5 to 200 mV s^{-1} (*dashed lines*—the theoretical Randles–Ševcik plots, noted in the figure)

Table 1 The media-specific parameters

Media	Dsys/cm^2 s^{-1}	$c$sys/mM
0.1 M KOH electrolyte [26–30]	1.8×10^{-5}	1.13
Nafion® ionomer [46]	9.95×10^{-7}	9.34
PVA ionomer [47]	1.8×10^{-5}	0.019

and oxygen concentration (c_{sys}) are the media-specific parameters; therefore, three theoretical lines taking into account the respective D_{sys} and c_{sys} values (Table 1) in the 0.1 M KOH solution [26–30], Nafion® [46] or PVA ionomer [47] have been constructed (dashed lines, inset in Fig. 5).

The experimental I_{peak} vs. $v^{1/2}$ plot for 5%PVA-Vulcan electrode coincides approximately with the constructed theoretical line for KOH solution, indicating that the dissolved oxygen in the electrolyte solution (0.1 M KOH) determines mainly the diffusion process characteristics for 5%PVA-Vulcan system. Increased ionic conductivity of the system refers to the interaction between the PVA ionomer and KOH electrolyte solution [19]. In contrast, the experimental I_{peak} vs. $v^{1/2}$ plot for 5%Nafion-Vulcan electrode is shifted from the constructed KOH theoretical line as well as from the Nafion® theoretical line. This refers to the influence of another parameter, namely the effective electrochemical surface area (S_{eff}) which probably differs from the geometric surface area of the glassy carbon electrode (S).

Although, the Randles–Ševcik equation is valid only for energetically homogeneous and geometrically flat electrode surfaces rather than for porous systems, Ward and Compton [22] simulated the voltammetry data for the porous electroactive surfaces and the Randles–Ševcik equation analysis was justified in the limit of low electrode potential scan rates [21, 22]. The Randles–Ševcik equation was used to analyse the differences between the electrode geometric surface area (S) and effective electrochemical surface area (S_{eff}) values. It should be mentioned that the calculated S_{eff} value can be used only as an approximate parameter for comparison of different systems under study. The calculated S_{eff} value for 5%PVA-Vulcan material is approximately equal to S, indicating that the 5%PVA-Vulcan catalyst behaves more like a flat electrode. The estimated effective electrochemical surface area value for the 5%Nafion-Vulcan is about 3 times higher than that for 5%PVA-Vulcan. This result shows that the surface of the 5%Nafion-Vulcan electrode is macroscopically rough and energetically inhomogeneous, and therefore, the rate of the electrochemical reactions depends on the surface region, where the reduction of O_2 or intermediates takes place [48–52]. Thus, the non-linear Poisson–Boltzmann theory [48], taking into account the effective Debye screening length (depending on the surface charge density (being different at various surface areas, i.e. sp^2 or sp^3 carbon areas)), should be introduced into complex models discussed in Refs. 22, 53.

Influence of Nafion® ionomer amount in the catalyst on ORR characteristics

The optimisation of the Nafion® ionomer amount in a catalyst is carbon specific; therefore, in this work, the CDC powder and Pt/CDC catalysts intermixed with different Nafion® amounts (5, 20, 30 and 50 wt%) were studied in 0.1 M KOH solution and compared with 5%Nafion-Vulcan electrode data, applying the RDE method (Figs. 6 and 7). As presented in Fig. 6., the ORR kinetic and the diffusion current densities for 5%Nafion-CDC are noticeably higher than those for the 5%Nafion-Vulcan electrode due to the well-developed meso-microporosity in the CDC-based electrode. In addition, it was established that the 20 or 30 wt% Nafion® amount in

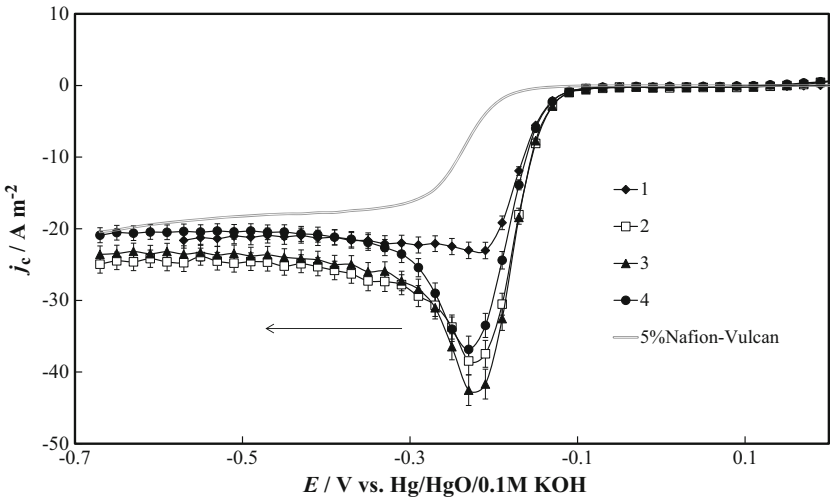

Fig. 6 RDE data for CDC electrodes with different Nafion® amounts: 5 wt% (*1*), 20 wt% (*2*), 30 wt% (*3*) and 50 wt% (*4*) in 0.1 M KOH solution saturated with O_2 (ν = 10 mV s^{-1}, ω = 500 rev min^{-1})

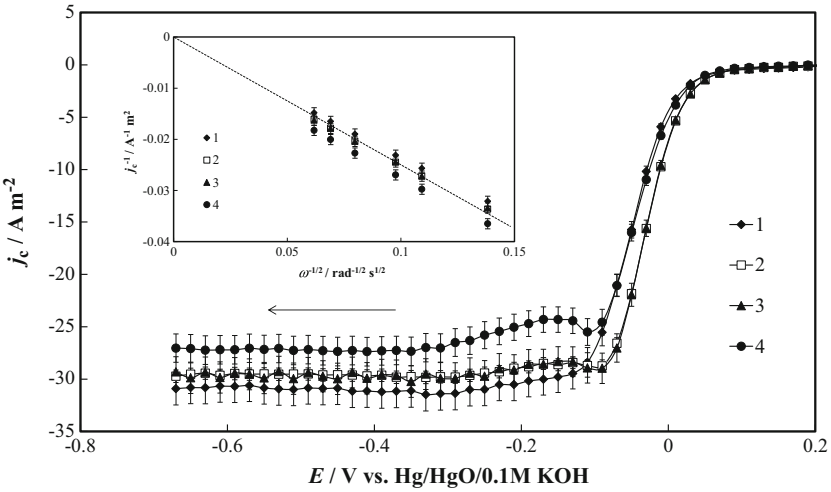

Fig. 7 RDE data for Pt/CDC catalysts with different Nafion® amounts: 5 wt% (*1*), 20 wt% (*2*), 30 wt% (*3*) and 50 wt% (*4*) in 0.1 M KOH solution saturated with O_2 (ν = 10 mV s^{-1}, ω = 500 rev min^{-1}). *Inset*: Koutecky-Levich plots calculated from RDE data for same catalysts at E = −0.41 V vs. Hg|HgO|0.1 M KOH (*dashed line*—the theoretical plot for a four electron transfer process of ORR)

the catalyst is optimal for the unmodified (Fig. 6) and also for the Pt nanoparticles modified (Fig. 7) CDC-based electrodes. Thus, the established results for CDC-based catalysts coincide with the data given in literature [8, 9].

j_c^{-1} vs. $\omega^{-1/2}$ plots for Pt/CDC catalysts mixed with different Nafion® amounts are very similar and coincide with the theoretically calculated Koutecky–Levich plot (n = 4, D_{sys} = 1.8 × 10^{-5} cm^2 s^{-1}and c_{sys} = 1.13 mM) (given inset in Fig. 7), indicating that four electron transfer process of ORR is valid for all Pt/CDC catalysts studied.

The Tafel-like relationships for various systems are presented in Fig. 8. The slope values of the Tafel-like plots calculated for the unmodified (−60 ± 3 mV dec^{-1}) and Pt nanoparticles modified (−81 ± 3 mV dec^{-1}) CDC catalysts are practically independent of the Nafion® amount in the catalyst within the low current density region. Thus, the rate determining step of ORR for CDC and Pt/CDC electrodes is not influenced by the Nafion® amount used [54]. According to the several authors [55–57], the Tafel-like slope value of −120 mV dec^{-1} indicates that the Langmuir mechanism is valid and thus, the first electron transfer is the rate determining step of ORR. The slope value of Tafel-like plots −60 mV dec^{-1}, however, follows the Temkin isotherm behaviour and the rate determining step for ORR is the multiple-electron transfer process. The slope values for Tafel-like plots −81 ± 3 mV dec^{-1} indicate the more complicated ORR mechanism for Pt/CDC electrodes.

It is interesting to mention that similarly, the value of the electrochemically active surface area 17 ± 1 m^2 g $_{Pt}^{-1}$ calculated from the cycling voltamogramms (ν = 5 mV s^{-1}) for the Pt/CDC catalyst with different amount of intermixed Nafion® is independent of the amount of the ionomer used in the catalyst ink. However, slight influence of the electrochemically active surface area due to differences in the lengths or

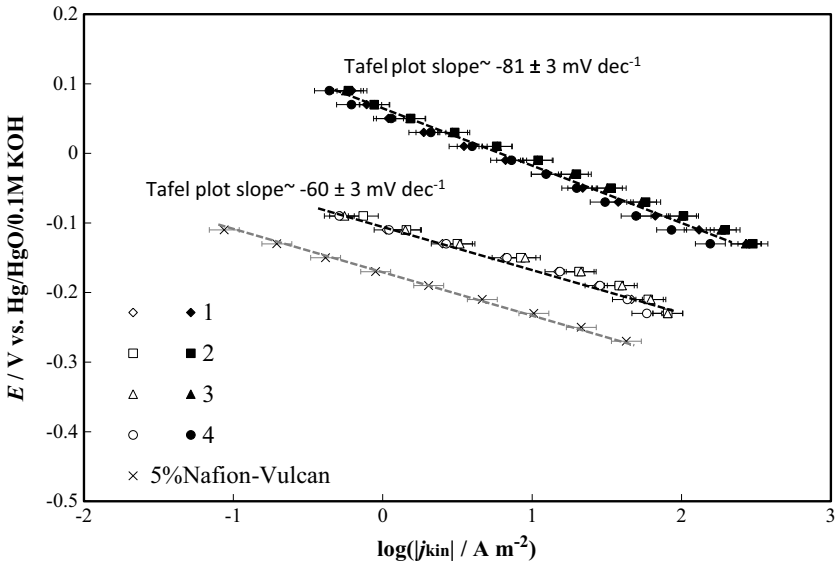

Fig. 8 Tafel-like plots constructed for Pt/CDC (*filled marks*) and CDC (*open marks*) systems with different Nafion® amounts: 5 wt% (*1*), 20 wt% (*2*), 30 wt% (*3*) and 50 wt% (*4*), and 5%Nafion-Vulcan for comparison

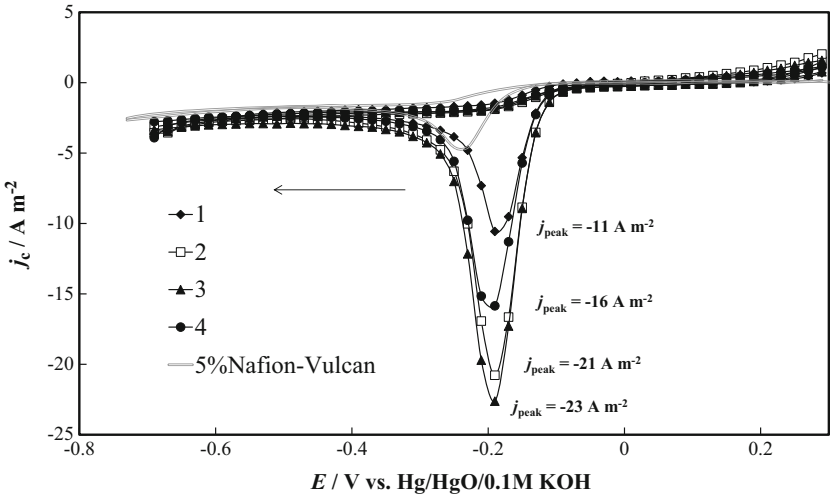

Fig. 9 Cyclic voltammograms for CDC electrodes with different Nafion® amounts: 5 wt% (*1*), 20 wt% (*2*), 30 wt% (*3*) and 50 wt% (*4*), and 5%Nafion-Vulcan for comparison in 0.1 M KOH solution saturated with O_2 (ν = 5 mV s^{-1})

structures of the same ionomer has been reported by Park et al. [11] being somewhat lower for the long-side chains of ionomer (57 m^2 g_{Pt}^{-1}) compared to that for the short-side chains of ionomer studied in acidic media.

According to the cyclic voltammetry data, the reduction peak potential value E_{peak} = −0.19 ± 0.01 or −0.04 ± 0.01 V (vs. Hg|HgO|0.1 M KOH) for CDC or Pt/CDC systems, respectively, is independent of the Nafion® amount in the catalyst (Figs. 9 and 10). However, the absolute value of the reduction peak current density ($|j_{peak}|$) depends on the Nafion® amount in the CDC and Pt/CDC systems, achieving a maximum for the 30 wt% of the Nafion® amount in the catalyst. CV and RDE methods confirm that the 30 wt% of the Nafion® amount in a catalyst provides the highest electrochemical activity toward ORR. It is important to mention that $|j_{peak}|$ for 30%Nafion-CDC system is significantly higher than that observed for 30%Nafion-Pt/CDC catalyst, probably caused by the different electrical double layer properties of the electrode surface. On the other hand, Menshykau et al. [23] demonstrated a significant effect of the electrode roughness on the shape of cyclic voltammograms and peak currents only at relatively high values of electrode roughness. In that sense, a further analysis of the Randles–Ševcik plots for 30%Nafion-CDC and 30%Nafion-Pt/CDC systems was conducted, and the results deviate remarkably from the constructed KOH theoretical lines, taking into account either two or four electron transfer mechanism per one oxygen molecule (Fig. 11). The calculated S_{eff} values (according to Eq. 1) increase in the following sequence: 5%Nafion-Pt/CDC ≤ 50%Nafion-Pt/CDC ≤ 20%Nafion-Pt/CDC ≈ 30%Nafion-Pt/CDC << 5%Nafion-CDC < 50%Nafion-CDC < 20%Nafion-CDC < 30%Nafion-CDC system, being higher than the geometric area of the glassy carbon substrate electrode (S = 0.196 cm^2). A similar tendency has been observed for systems described in our previous works [25–29].

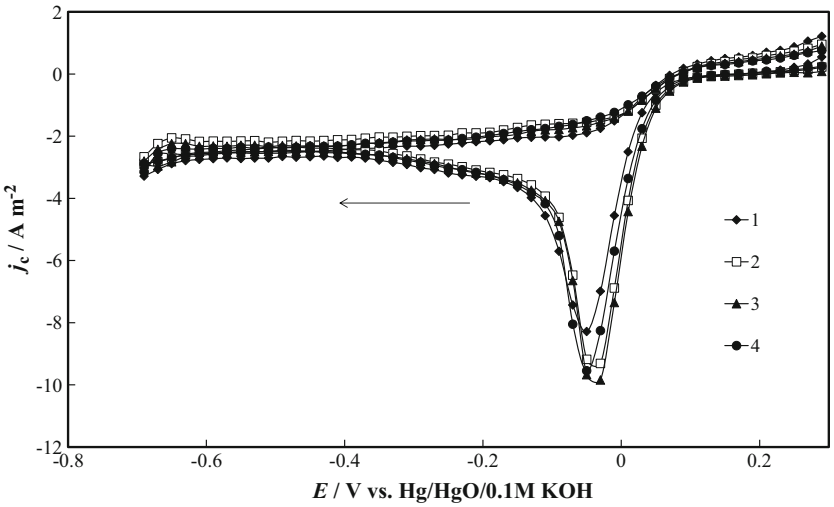

Fig. 10 Cyclic voltammograms for Pt/CDC electrodes with different Nafion® amounts: 5 wt% (*1*), 20 wt% (*2*), 30 wt% (*3*) and 50 wt% (*4*) in 0.1 M KOH solution saturated with O_2 (ν = 5 mV s^{-1})

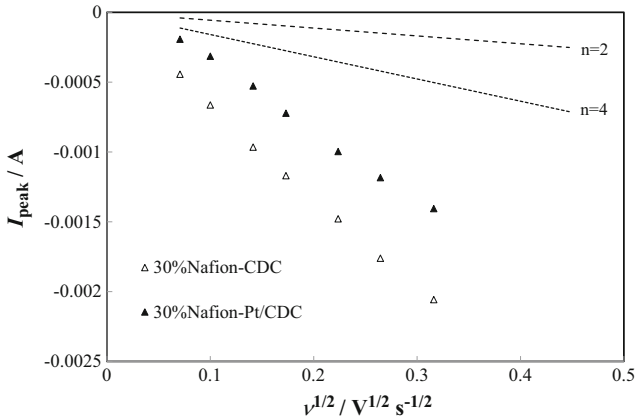

Fig. 11 Randles–Ševcik plots for various electrodes, noted in the figure: *dots*—studied systems and *dashed lines*—theoretical Randles–Ševcik plots for two or four electrons transferred per one oxygen molecule

Comparison of catalyst activity toward ORR

The determined electrode potential values for all catalysts studied at the constant current density (j_c = 10 A m^{-2}), ω = 500 rev min^{-1} and ν = 10 mV s^{-1}) have been given in Fig. 12. The diagram demonstrates that more positive electrode potential values have been obtained for 20%Nafion-Pt/CDC and 30%Nafion-Pt/CDC, indicating that the Pt/CDC catalyst with the optimum amount of Nafion® ionomer provides the higher activity, i.e. the higher number of the triple phase boundaries, and therefore, has a higher electrochemical activity toward ORR [27, 29]. Similarly, to our work, Park et al. [11, 12] have shown the importance of the uniform and continuous ionomer coverage over the surfaces of the Pt particles and carbon support in order to improve the efficiency of the ORR.

It is important to mention that the optimisation of Nafion® amount in the catalysts has noticeably lower effect on the electrode potential value compared with the case if the carbon support (CDC vs. Vulcan) or ionomer (PVA vs. Nafion®) has been replaced. The major change in the electrode potential value is caused either by modification of the CDC support with the Pt nanoparticles (~130 mV shift toward less negative electrode potentials) or by replacing PVA with Nafion® ionomer in the Vulcan-based system (~140 mV shift).

Conclusion

The polyvinyl alcohol (PVA) or Nafion® ionomer-based catalysts have been studied using various physical and electrochemical characterisation methods. The electrochemical activity toward ORR of the catalysts in oxygen-saturated 0.1 M KOH aqueous solution noticeably depends on the chemical composition of the binder (PVA or Nafion®).

The variation of the amount of the Nafion® ionomer intermixed with CDC or Pt/CDC catalysts influences the ORR kinetics. The highest electrochemical activity toward ORR was established for 30%Nafion-Pt/CDC catalyst due to the higher number of electrochemically active sites in the catalyst surface. The calculated electrochemically active surface area values for the Pt/CDC catalysts are independent of the Nafion® amount intermixed in the catalyst ink.

We also conclude that the variation of the Nafion® amount in the catalyst has a moderate effect compared to the influence of replacing either the carbon support (CDC vs. Vulcan) or ionomer (PVA vs. Nafion®).

A significant effect on the ORR peak current values in cyclic voltammograms was observed and the estimated S_{eff} values for all catalyst systems (except for 5%PVA-Vulcan) were higher than the geometric area of the glassy carbon electrode.

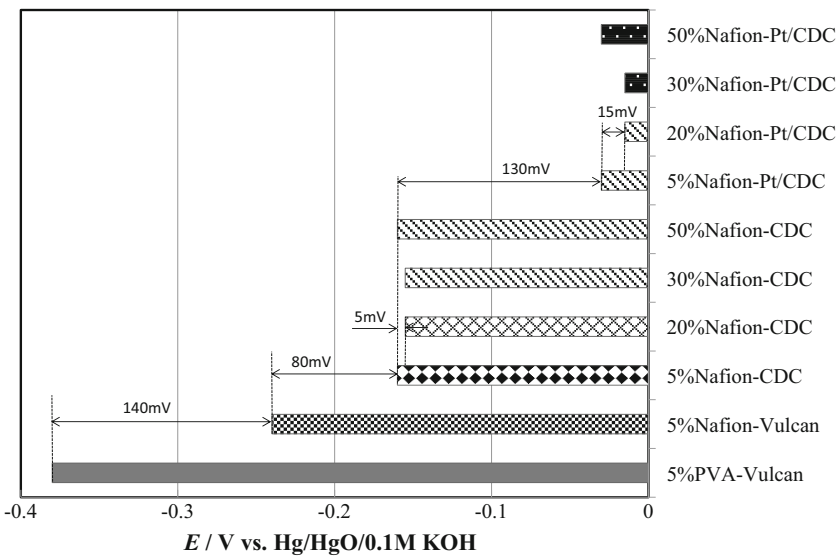

Fig. 12 The obtained electrode potential values (*E* vs. Hg|HgO|0.1 M KOH) at the constant current density for various systems studied (j_c = 10 A m^{-2}, ω = 500 rev min^{-1}, ν = 10 mV s^{-1}), noted in Figure

Acknowledgements This work was supported by the European Spallation Source Project: Estonian Partition in ESS Instrument design, development; building and application for scientific research: SLOKT12026T, the Estonian institutional research grant No. IUT20-13, the Estonian Centre of Excellence in Science: TK117T "High-technology Materials for Sustainable Development", the European Regional Development Fund: TK141 "Advanced materials and high-technology devices for energy recuperation systems", the Estonian Energy Technology Program: SLOKT10209T, the Materials Technology Project: SLOKT12180T, NAMUR "Nanomaterials—research and applications" (3.2.0304.12-0397), and by personal research grant No. PUT55. The authors would like to thank Dr. Karmen Lust for providing critical comments and English corrections of the manuscript.

References

1. Wilson MS, Valerio JA, Gottesfeld S (1995) Low platinum loading electrodes for polymer electrolyte fuel cells fabricated using thermoplastic ionomers. Electrochim Acta 40(3):355–363
2. Jung HY, Cho KY, Sung KA, Kim WK, Kurkuri M, Park JK (2007) Sulfonated poly (arylene ether sulfone) as an electrode binder for direct methanol fuel cell. Electrochim Acta 52:4916–4921
3. Holdcroft S (2014) Fuel cell catalyst layers: a polymer science perspective. Chem Mater 26:381–393
4. Antolini E, Giorgi L, Pozio A, Passalacqua E (1999) Influence of Nafion loading in the catayst layer of gas-diffusion electrodes for PEFC. J Power Sources 77:136–142
5. Viswanathan B, Helen M (2007) Is Nafion the only choice? Bulletin of the Catalysis Society of India 6:50–55
6. Litster S, McLean G (2004) PEM fuel cell electrodes. J Power Sources 130:61–76
7. Zhang X-Y, Ding Y-H (2014) Thickness-dependent structural and transport behaviors in the platinum–Nafion interface: a molecular dynamics investigation. RSC Adv 4:44214–44222
8. Sasikumar G, Ihm JW, Ryu H (2004) Dependence of optimum Nafion content in catalyst layer on platinum loading. J Power Sources 132:11–17
9. Passalacqua E, Lufrano F, Squadrito G, Patti A, Giorgi L (2001) Nafion content in the catalyst layer of polymer electrolyte fuel cells: effects on structure and performance. Electrochim Acta 46:799–805
10. Antoine O, Bultel Y, Durand R (2001) Oxygen reduction reaction kinetics and mechanism on platinum nanoparticles inside Nafion®. J Electroanal Chem 499:85–94
11. Park Y-C, Kakinuma K, Uchida H, Watanabe M, Uchida M (2015) Effects of short-side-chain perfluorosulfonic acid ionomers as binders on the performance of low Pt loading fuel cell cathodes. J Power Sources 275:384–391
12. Park Y-C, Tokiwa H, Kakinuma K, Watanabe M, Uchida M (2016) Effects of carbon supports on Pt distribution, ionomer coverage and cathode performance for polymer electrolyte fuel cells. J Power Sources 315:179–191
13. Siroma Z, Fujiwara N, Ioroi T, Yamazaki S, Yasuda K, Miyazaki Y (2004) Dissolution of Nafion membrane and recast Nafion film in mixtures of methanol and water. J Power Sources 126:41–45
14. Jung HY, Cho KY, Lee YM, Park JK, Choi JH, Sung YE (2007) Influence of annealing of membrane electrode assembly (MEA) on performance of direct methanol fuel cell (DMFC). J Power Sources 163:952–956
15. Zook LA, Leddy J (1996) Density and solubility of nafion: recast, annealed, and commercial films. Anal Chem 68:3793–3796
16. Marten ML (2004) Encyclopedia of polymer science and technology, in: Kroschwitz JI (ed). 3rd edn. Wiley, New York Volume 8: 399–436
17. Ye Y-S, Rick J, Hwang B-J (2012) Water soluble polymers as proton exchange membranes for fuel cells. Polymers 4(2):913–963. doi:10.3390/polym4020913
18. Silva R, Muniz EC, Rubira AF (2008) Multiple hydrophilic polymer ultra-thin layers covalently anchored to polyethylene films. Polymer 49:4066–4075
19. Zugic DL, Perovic IM, Nikolic VM, SLJ M, Marceta Kaninski MP (2013) Enhanced performance of the solid alkaline fuel cell using PVA-KOH membrane. Int J Electrochem Sci 8:949–957
20. Masa J, Batchelor-McAuley C, Schuhmann W, Compton RG (2014) Koutecky-Levich analysis applied to nanoparticle modified rotating disk electrodes: electrocatalysis or misinterpretation? Nano Res 7(1):71–78
21. Ward KR, Gara M, Lawrence NS, Seth Hartshorne R, Compton RG (2013) Nanoparticle modified electrodes can show an apparent increase in electrode kinetics due solely to altered surface geometry: the effective electrochemical rate constant for non-flat and non-uniform electrode surfaces. J Electroanal Chem 695:1–9
22. Ward KR, Compton RG (2014) Quantifying the apparent 'Catalytic effect of porous electrode surfaces. J Electroanal Chem 724:43–47
23. Menshykau D, Streeter I, Compton RG (2008) Influence of electrode roughness on cyclic voltammetry. J Phys Chem C 112:14428–14438
24. Jänes A, Thomberg T, Kurig H, Lust E (2009) Nanoscale fine-tuning of porosity of carbide derived carbon prepared from molybdenum carbide. Carbon 47:23–29
25. Chai GS, Yoon SB, Yu J-S, Choi J-H, Sung Y-E (2004) Ordered porous carbons with tunable pore sizes as catalyst supports in direct methanol fuel cell. J Phys Chem B 108:7074–7079
26. Álvarez G, Alcaide F, Miguel O, Calvillo L, Lázaro MJ, Quintana JJ, Calderón JC, Pastor E, Esparbé I (2010) Technical electrodes catalyzed with PtRu on mesoporous ordered carbons for liquid direct methanol fuel cells. J Solid State Electrochem 14:1027–1034
27. Jäger R, Härk E, Steinberg V, Lust E (2016) Influence of temperature on the oxygen electroreduction activity at micro-mesoporous carbon support. J Electrochem Soc 163(3):F284–F290
28. Jäger R, Härk E, Kasatkin PE, Lust E (2014) Investigation of a carbon-supported Pt electrode for oxygen reduction reaction in 0.1 M KOH aqueous solution. J Electrochem Soc 161(9):F861–F867
29. Härk E, Jäger R, Lust E (2015) Effect of platinum nanoparticle loading on oxygen reduction at Pt Nanocluster activated microporous-mesoporous carbon support. Electrocatal 6:242–254
30. Härk E, Jäger R, Kasatkin PE, Steinberg V, Romann T, Möller P, Kanarbik R, Aruväli J, Kirsimäe K, Lust E (2015) Oxygen electrocatalysis on high-surface area non-Pt metal modified carbon catalysts. ECS Trans 64(36):11–21
31. Zhang J, Tang S, Liao L, Yu W, Li J, Seland F, Haarberg GM (2014) Improved catalytic activity of mixed platinum catalysts supported on various carbon nanomaterials. J Power Sources 267:706–713
32. Seah MP, Gilmore IS, Spencer SJ (2001) Quantitative XPS: I. Analysis of X-ray photoelectron intensities from elemental data in a digital photoelectron database. J Electron Spectrosc Relat Phenom 120:93–111
33. Fairley N, CasaXPSversion 2.3.12 www.casaxps.com
34. Datsyuk V, Kalyva M, Papagelis K, Parthenios J, Tasis D, Siokou A, Kallitsis I, Galiotis C (2008) Chemical oxidation of multiwalled carbon nanotubes. Carbon 46:833–840
35. Diaz J, Paolicelli G, Ferrer S, Comin F (1996) Separation of the sp3 and sp2 components in the C1s photoemission spectra of amorphous carbon films. Phys Rev B Condens Matter 54:8064–8069

36. Payne BP, Biesinger MC, McIntyre NS (2011) X-ray photoelectron spectroscopy studies of reactions on chromium metal and chromium oxide surfaces. J Electron Spectrosc Relat Phenom 184:29–37
37. Beverly S, Seal S, Hong S (2000) Identification of surface chemical functional groups correlated to failure of reverse osmosis polymeric membranes. J Vac Sci Technol 18:1107–1113
38. Chen C, Levitin G, Hess DW, Fuller TF (2007) XPS investigation of Nafion® membrane degradation. J Power Sources 169(2):288–295
39. Joo JB, Kim YJ, Kim W, Kim P, Yiet J (2008) Simple synthesis of graphitic porous carbon by hydrothermal method for use as a catalyst support in methanol electro-oxidation. Catal Commun 10(3): 267–271
40. DeLuca NW, Elabd YA (2006) Nafion®/poly (vinyl alcohol) blends: effect of composition and annealing temperature on transport properties. J Membrane Science 282:217–224
41. Jiang L, Hsu A, Chu D, Chen R (2009) Oxygen reduction on carbon supported Pt and PtRu catalysts in alkaline solutions. J Electroanal Chem 629:87–93
42. Macià MD, Campiña JM, Herrero E, Feliu JM (2004) On the kinetics of oxygen reduction on platinum stepped surfaces in acidic media. J Electroanal Chem 564:141–150
43. Kuzume A, Herrero E, Feliu JM (2007) Oxygen reduction on stepped platinum surfaces in acidic media. J Electroanal Chem 599:333–343
44. Grozovski V, Kasuk H, Nerut J, Härk E, Jäger R, Tallo I, Lust E (2015) Oxygen reduction at shape-controlled platinum nanoparticles and composite catalysts based on (100)Pt nanocubes on microporous–mesoporous carbon supports. ChemElectroChem 2:847–851
45. Paulus UA, Wokaun A, Scherer GG, Schmidt TJ, Stamenkovic V, Markovic NN, Ross PN (2002) Oxygen reduction on high surface area Pt-based alloy catalysts in comparison to well defined smooth bulk alloy electrodes. Electrochim Acta 47:3787–3798
46. Parthasarathy A, Srinivasan S, Appleby AJ, Martin CR (1992) Temperature dependence of the electrode kinetics of oxygen reduction at the platinum/nafion® Interface—a microelectrode investigation. J Electrochem Soc 139(9):2530–2537
47. Marek P, Velasco-Veléz JJ, Doll T, Sadowski G (2014) Compensation for the influence of temperature and humidity on oxygen diffusion in a reactive polymer matrix. J Sens Sen Syst 3: 291–303
48. Daikhin LI, Kornyshev AA, Urbakh M (1998) Nonlinear Poisson-Boltzmann theory of a double layer at rough metal/electrolyte interface: a new look on the capacitance data on solid electrodes. J Chem Phys 108:1715–1723
49. Daikhin LI, Kornyshev AA, Urbakh M (1996) Double-layer capacitance on a rough metal surface. Phys Rev E 53:6192–6199
50. Lust E, Jänes A, Sammelselg V, Miidla P, Lust K (1998) Surface roughness of bismuth, antimony and cadmium electrodes. Electrochim Acta 44:373–383
51. Lust E, Jänes A, Sammelselg V, Miidla P (2000) Influence of charge density on the electrochemical surface roughness of cadmium electrode. Electrochim Acta 46:185–191
52. Lust E, Kallip S, Möller P, Jänes A, Sammelselg V, Miidla P, Väärtnõu M, Lust K (2003) Influence of surface charge density on the electrochemical surface "roughness" of Bi electrodes. J Electrochem Soc 150:E175–E184
53. Collier CP, Saykally RJ, Shiang JJ, Henrichs SE, Heath JR (1997) Reversible tuning of silver quantum dot monolayers through the metal-insluator transition. Science 277(5334):1978–1981
54. Shinagawa T, Garcia-Esparza AT, Takanabe K (2015) Insight on Tafel slopes from a microkinetic analysis of aqueous electrocatalysis for energy conversion. Scientific Reports 5(13801):1–21
55. Zhang J (Ed) (2008) PEM fuel cell electrocatalysts and catalyst layers fundamentals and applications, Springer-Verlag, London Limited pp 89–134
56. Gómez-Marín AM, Rizo R, Feliu JM (2013) Some reflections on the understanding of the oxygen reduction reaction at Pt(111). Beilstein J Nanotechnol 4:956–967
57. Perez J, Gonzalez ER, Ticianelli EA (1998) Oxygen electrocatalysis on thin porous coating rotating platinum electrodes. Electrochim Acta 44(8–9):1329–1339